JOURNAL OF MATERIALS SCIENCE 25 (1990) 4106-4112

Ageing of dealloyed copper

A. D. TOMSETT, D. J. YOUNG, M. R. STAMMBACH, M. S. WAINWRIGHT
School of Chemical Engineering and Industrial Chemistry, The University of New South Wales, P.O. Box 1, Kensington, New South Wales 2033, Australia

A finely divided copper rod structure has been prepared by the selective dissolution of aluminium from a Cu–50 wt% Al alloy in aqueous NaOH. The aging behaviour of this product has been studied by measurement of the coarsening of the pore and copper rod structure. A decrease in caustic concentration or temperature was found to reduce the rate of coarsening. The leaching reaction was found to play no part in the coarsening process. A dissolution–reprecipitation mechanism, where copper dissolves from faults within the structure and reprecipitates on adjacent copper rods was found to account quantitatively for the development of the coarsening process in its early stages. However, this model breaks down after extended times when the rod geometry is destroyed.

1. Introduction

The dissolution in alkali of aluminium from appropriate intermetallic phases to produce a porous metal residue is a well known phenomenon, and has been used to produce high surface area metal catalysts for many years [1]. The particular example of $CuAl_2$ dealloying has been shown [2, 3] to proceed at ambient temperatures via selective dissolution

$$CuAl_2(s) + 2OH^-(aq) + 6H_2O = 2Al(OH)_4^-(aq) + 3H_2(g) + Cu(s) \quad (1)$$

In this case the copper rearranges to form its new morphology without itself dissolving. The nature of this rearrangement is of interest because, although two thirds of the solid's atoms are lost, its external dimensions are unchanged. The reaction product is highly porous, and the pores have been found [4] to be very fine, of order 20 to 100 nm.

Two diffusion processes contribute to the reaction morphology [3, 5]. Aluminium is removed, and leachant $OH^-(aq)$ supplied, by diffusion through the liquid phase occupying the pores. This process controls the reaction rate, and the product zone thickness, X, increases with time, t, according to parabolic kinetics

$$X^2 = k_p t \quad (2)$$

The second diffusion process permits segregation of the copper and aluminium from the parent alloy toward the advancing copper and pore liquid phases at the reaction front. The spacing of the product (copper plus pore) structure is controlled by boundary diffusion along the $CuAl_2$–product interface and can be related by cellular phase transformation theory to the rate at which this interface advances [5]. The cellular nature of the product has been verified by electron microscopy [6] which also revealed that the pore space constitutes a continuous region and the copper exists as cylindrical fibres. Further confirmation is provided by the finding [4] that the pores are parallel-sided.

Although the kinetics and morphological development of the initial dealloying process are accurately described by this combination of liquid and solid-state diffusion, the description is incomplete. The solubility of copper in alkali is low, but not zero, and a high surface area structure cannot have long term stability in this environment. In fact, a decrease in total surface area with time has been observed after long periods of dealloying [7, 8] but no explanation has ever been advanced for this phenomenon.

The purpose of the present work was to examine the kinetics of this coarsening process and the effects thereon of variations in reaction conditions.

2. Experimental procedure

A Cu–50 wt % Al alloy was prepared by induction melting, casting the melt into heated moulds, and cutting the resulting 5.4 mm diameter rods into 5 mm lengths with a low speed saw. The alloy was almost entirely composed of the phase $CuAl_2$, with some interdentritic frozen eutectic. Its microstructure is shown in Fig. 1.

Reaction kinetics were studied by leaching pellets in a very large excess of a 20 wt % aqueous NaOH solution at 274, 283, 301 and 323 K. The reaction was terminated at different time periods by washing with distilled water to produce pellets with varied depth of caustic attack. These were mounted in a cold setting resin, cross-sectioned and polished to a 1 μm finish. The depth of chemical attack was measured under an optical microscope using a micrometer eyepiece.

The aging in caustic solution of copper leach residues was studied as follows. Rods were leached in a large excess of 20 wt % NaOH solution for either 1 h at 323 K or 90 h at 274 K. The copper rims, which were 0.02 cm thick when leached at 323 K, and 0.063 cm thick when leached at 274 K, were then mechanically

0022–2461/90 $03.00 + .12

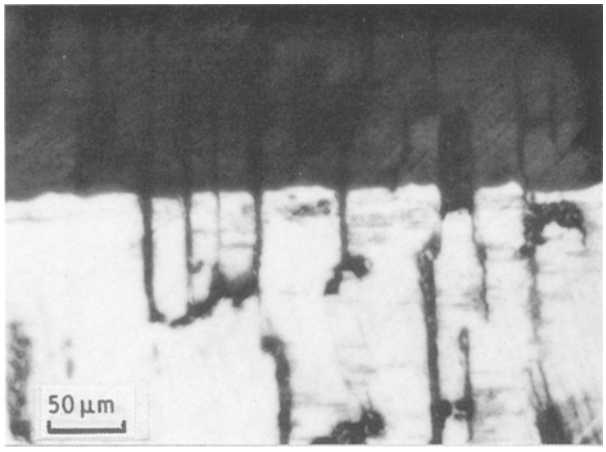

Figure 1 Micrograph of section through partially leached Al–50Cu alloy.

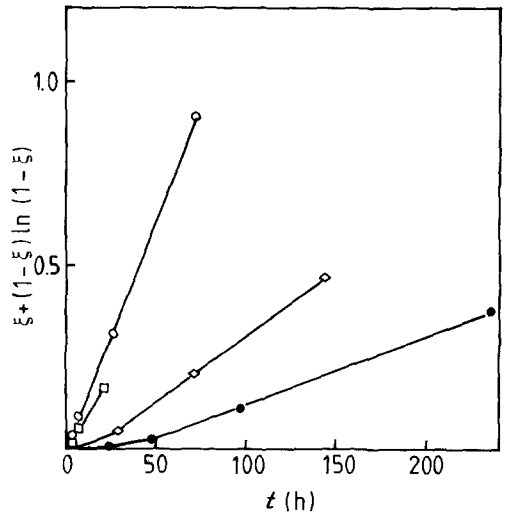

Figure 2 Leaching kinetics plotted according to Equation 3. (● 274 K, ◇ 283 K, □ 301 K, ○ 323 K).

removed from the alloy core and washed with a fresh 20% NaOH solution to remove residual aluminate. Small portions of this copper (about 1 g) were then placed in fresh aqueous NaOH solution. Aging experiments were conducted in the temperature range 274 to 366 K, with aqueous NaOH concentrations of from 0 to 20 wt %. Samples were aged in these solutions for different periods and then characterized according to their surface areas, pore volumes, pore size distributions and copper crystallite sizes.

The BET surface areas of the copper rims were measured using a single-point chromatographic technique [9]. The pore size distributions and total pore volumes of the copper rims were determined, after passivation by nitrous oxide [10], by mercury porosimetry using a Micromeritics Autopore 9200 mercury intrusion porosimeter. The copper crystallite size was estimated from the line broadening of the Cu(1 1 1) and (2 0 0) X-ray diffraction lines using the Scherrer equation. Corrections for instrumental broadening were obtained from the silicon (2 2 0) diffraction line. As the copper is pyrophoric, the samples were coated in collodion prior to examination, and the analysis was carried out under a nitrogen atmosphere. The compositions of the leach residue and the dissolved copper concentration of the NaOH solutions were determined by atomic absorption spectrometric analysis.

3. Results

The general appearance of the dealloyed material is shown in Fig. 1. The accurate reproduction of the prior alloy structure in the leach residue is apparent. The leaching kinetics are shown in Fig. 2, plotted according to the equation [11] for diffusion control through a reaction product rim with cylindrical geometry

$$t/\tau = \xi + (1 - \xi) \ln (1 - \xi) \quad (3)$$

where

$$\xi = 1 - (r_c/R_0)^2 \quad (4)$$

where, τ is the time required for complete reaction, R_0 the initial radius of the cylinder and r_c the radius of the remnant alloy core. It is seen that after an initial period the kinetic data conform closely with the predictions of the diffusion model.

Copper residues produced at 274 K were aged in 20 wt % NaOH solution at several different temperatures. Copper crystallite sizes were found to increase, as shown in Fig. 3, the average growth rate increasing with temperature. Copper crystallite growth was accompanied by a coarsening in average pore size and, at higher temperatures, a broadening of pore size distribution. These effects are shown in Fig. 4, where an apparent steady-state is seen to be approached at long aging times. Gas adsorption measurements showed that the volume fraction of pore space in the residue was constant at 0.64 during aging, but the surface area decreased from its initial value of 18.7 $m^2 g^{-1}$ until a constant value was reached. A decrease in surface area at constant pore volume implies an increase in pore size and spacing. This observation was therefore consistent with the crystallite size and pore radius measurements and confirmed that a steady-state was reached. The higher the aging temperature, the coarser was the steady-state structure: lower surface area, larger pore radii and crystallite sizes. The rate of approach to the steady-state surface

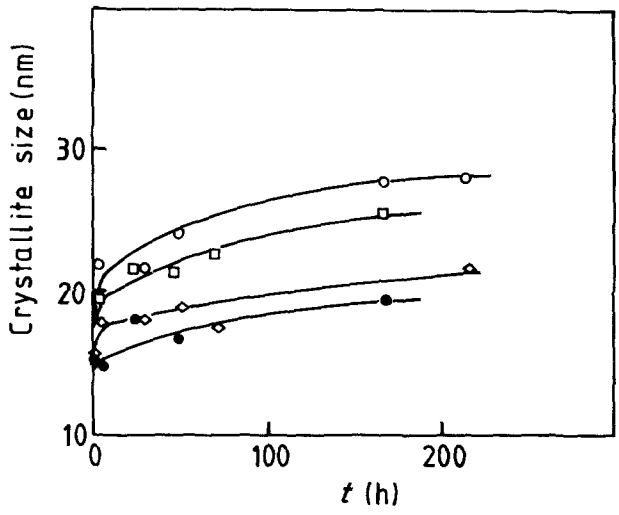

Figure 3 Variation of copper crystallite size during aging of reaction product leached at 274 K. (● 274 K, ◇ 283 K, □ 301 K, ○ 323 K).

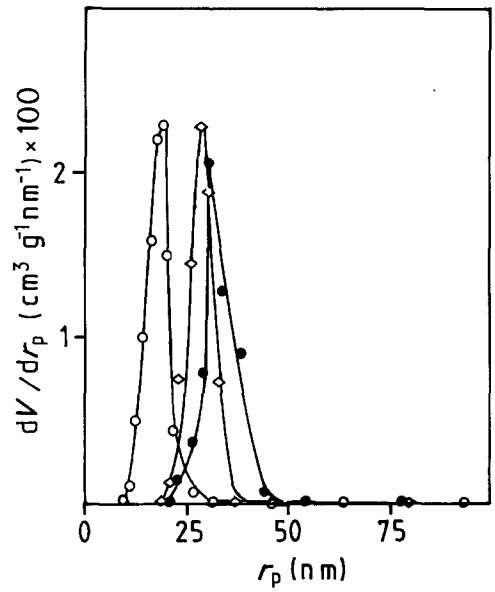

Figure 4 Evolution of pore size distributions during aging at 274 K of a residue produced by leaching at 274 K. (○ 0 h, ◇ 50 h, ● 168 h).

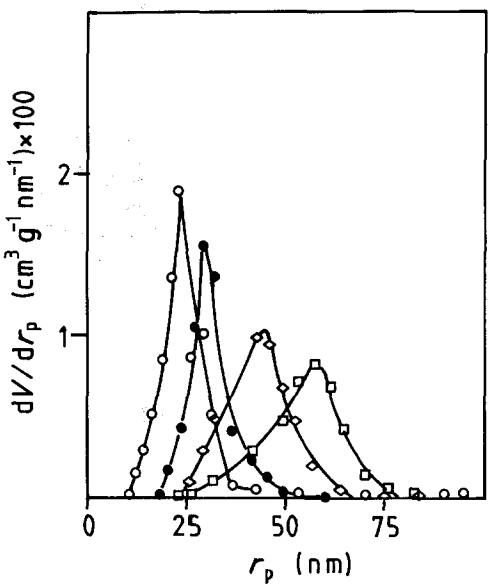

Figure 5 Variation of apparent pore size distribution during aging of reaction product leached at 323 K. Aging temperature was 366 K. (○ 0 h, □ 1 h, ◇ 18 h, ● 162 h).

area value increased with increasing temperature. Steady-state morphologies are described in Table I.

Copper residues produced by leaching at 323 K were also found to coarsen during subsequent aging. Copper crystallite size measurements were subject to considerable scatter, but yielded several qualitative results. Aging at 323 K produced no measurable effect in NaOH concentrations of 0 and 0.1 wt %, but significant coarsening rates at concentrations of 1 and 20 wt %. Aging in 20 wt % NaOH produced no coarsening at the lower temperature of 283 K, but significant coarsening at 366 K. Where coarsening occurred, an apparent steady-state was reached after about 100 h.

Pore size measurements on aged residues of a 323 K leaching process led to results which were at variance with the crystallite size measurements. An example is shown in Fig. 5, where the average pore size is seen first to increase and then decrease with the passage of time. However, gas adsorption measurements showed the pore volume fraction to be approximately constant at 0.64, whilst the surface area decreased from its initial value of 15.5 $m^2 g^{-1}$ and approached a constant value. The surface area measurements are consistent with the monotonic coarsening process reflected in the crystallite size measurements, but in disagreement with the porosimetry results. Since pore volume and surface area measurements are made without reference to any assumed sample morphology, they are generally reliable. On the other hand, pore sizes calculated from mercury intrusion measurements rely on an assumption as to the pore shape, in this case that of parallel-sided pores. The apparent reversal in direction of charge in mean pore radius, which is inconsistent with the surface area, pore volume and crystallite size measurements, therefore indicates a change in pore morphology. This change was observed after aging times which became shorter as the aging temperature was increased. Steady-state values of morphological variables are listed in Table II.

Chemical analysis revealed that aluminium levels in the leach residues were initially 1.6 ± 0.2% when dealloyed at 274 K and 1.2 ± 0.1% when dealloyed at 323 K. Aging led to some decrease in these levels until a steady-state was reached. Final values are shown in Tables I and II. Dissolved copper concentrations in the aging solutions rose quickly to a level which remained approximately constant. These levels are stated in Tables I and II.

4. Discussion

The present results show very clearly that the morphology of a copper dealloying residue can change during immersion in alkali solution subsequent to the cessation of the leaching reaction. Earlier work [7] has shown that such changes can be observed whilst the leaching reaction is still in progress. The two observations may be compared as follows. Copper crystallite sizes were measured for pre-leached and mechanically

TABLE I Steady-state quantities after aging in 20% NaOH of residues produced at 274 K

Aging temperature (K)	Surface area ($m^2 g^{-1}$)	Pore radius* (nm)	Crystallite size (nm)	Al (wt %)	Cu(aq) (ppm)
Before aging	18.7	18	15	1.6	0
274	13.9	30	20	0.8	5
283	11.6	32	21	0.7	2
301	11.0	37	25	0.5	4
323	7.7	61	27	0.5	2

*Taken at maximum in dV/dr_p against r_p plot.

TABLE II Steady-state quantities after aging residues produced at 323 K

Aging temperature (K)	NaOH (wt %)	Surface area ($m^2 g^{-1}$)	Crystallite size (nm)	Al (wt %)	Cu(aq) (ppm)
Before aging		15.5	22	1.2	–
323	1	10.4	28	0.6	2
323	20	7.4	30	0.4	3
283	20	13.5	22	0.6	2
366	20	7.9	30	0.4	13

TABLE III Calculation of pore sizes after aging of material leached at 274 K

T (K)	t (h)	DC^* (10^{12} mol cm^{-1} sec^{-1})	r_p(max)	
			Observed* (nm)	Calculated (nm)
274	50	0.7	24	24
274	168	0.7	29	29
283	53	2.2	22	22
283	72	2.2	35	35
283	169	2.2	35	57
301	3	3.0	20	20
301	46	3.0	36	36
301	166	3.0	37	56
323	3	5.0	36	22
323	7	5.0	59	59
323	166	5.0	65	65

*Accuracy of experimental measurement better than 5%.

separated material during subsequent aging in alkali, and also [7] at the external surface of large samples whilst the leach reaction was continuing within those samples. Results are compared in Fig. 6 where it is seen that the process occurs at the same rate and reaches the same apparent steady-state in the two different cases. Evidently the leaching reaction itself plays no part in the crystallite enlargement process, and it follows that the morphological changes result solely from the interaction between the porous copper and its alkaline environment.

The magnitude of the changes during aging indicates that a fairly rapid mass transfer process occurs. The only mechanism available for such a process in the present system is liquid phase diffusion. The existence of a range of pore sizes within a single sample necessarily implies the simultaneous existence of copper surfaces having different curvatures and hence different solubilities. Thus a driving force exists for the dissolution of copper from regions of high curvature, i.e. from a finely divided, finely porous state, and for its reprecipitation at sites where a coarser morphology and hence a lower curvature exists. The significant concentrations of copper dissolved in the alkali solution shown in Tables I and II are consistent with such a mechanism. Other observations pointing to the operation of a dissolution–reprecipitation process are the general increase in pore coarsening rates with both temperature and alkali concentration.

In order to discuss the coarsening process, it is

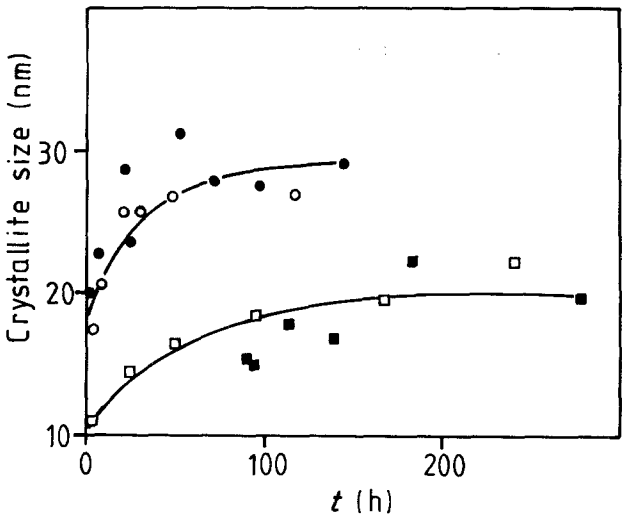

Figure 6 Comparison of crystallite size during aging of leached rims detached from the alloy (closed symbols) with those of the external surface of continuously leaching alloy samples [20] (open symbols). (□ 274 K, ○ 323 K).

necessary first to describe the initial size distribution of the structure when it is formed.

4.1. Initial size distribution

The nature of the pore size distribution prior to any ripening can be deduced from the kinetics of the cellular phase transformation which produced the pores. The spacing, S, of copper rods produced at the reaction front is shown schematically in Fig. 7. Because alloy segregation at the reaction front is controlled by boundary diffusion [5], the spacing is related to the rate at which the front advances through [12–16]

$$\frac{dx}{dt} = \frac{B}{S^3} \tag{5}$$

with

$$B = \frac{24 D_B \delta K}{aRT} \frac{f^{Cu} f^p \sigma}{C^{Cu} - C^p} \tag{6}$$

and D_B the boundary diffusion-coefficient, σ the boundary width, K the equilibrium constant for partition of solute copper between bulk $CuAl_2$ and boundary, a a geometrical constant of order unity, f^{Cu} and f^p are the volume fractions of the copper and pore phase, σ the surface energy of the copper-pore interface, C^{Cu} and C^p are solute concentrations in the product phases. If the residue's structure is unaltered after dealloying, combination of Equation 5 with the

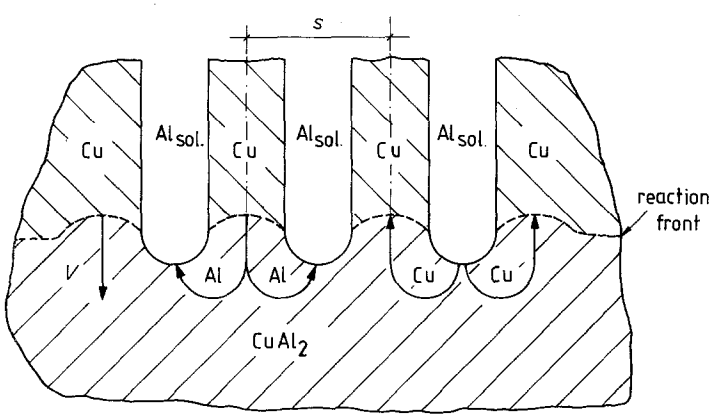

Figure 7 Schematic representation of $CuAl_2$–Cu interface during dealloying.

differential form of Equation 3 yields

$$S^3 = -4B\tau/R_0(1 - x/R_0)\ln(1 - x/R_0) \quad (7)$$

with x denoting the position within the rim relative to the external surface. The relationship between S and the measured pore radius can be calculated from the geometry of the residue's structure. If the copper rods are regularly spaced with their centres on a square grid, then the effective pore radius, r_p, as measured by gas adsorption or porosimetry [17] is calculated from the rod-to-rod distance along the grid diagonal as

$$2r_p = S[\sqrt{2} - 2(f_{Cu}/\pi)^{1/2}] \quad (8)$$

The copper rod radius r_{Cu} is

$$r_{Cu} = S(f_{Cu}/\pi)^{1/2} \quad (9)$$

and the number of rods per unit cross-sectional area is

$$N = 1/S^2 \quad (10)$$

Thus combination of Equations 7 to 10 permits calculation of pore and rod radii, together with N, as functions of position. We now verify the applicability of the above description in the absence of coarsening.

Aging at 274 K produces only very slow coarsening, as shown in Figs 3 and 4. It should, therefore, be possible to calculate the variation of pore size within a residue produced by dealloying at this temperature, on the basis that the copper rods, once formed, do not coarsen at all. Pore size distributions for a dealloyed sample are calculated by applying Equations 7 and 8 to small volume elements which in summation make up the entire sample. Concentric cylindrical shells were used as volume elements, and the values $\tau = 1.9 \times 10$ sec, $a = 1$, $f^{Cu} = 0.36$, $\sigma = 10^{-5}$ J cm^{-2}, $C^{Cu} = 0.13$ and $C^{p} = 0$ mol cm^{-3} were employed. Fitting the curve to porosimetry data obtained on a sample dealloyed at 274 K for 90 h yielded the results shown in Fig. 8, and the estimate $D_B\delta K = 7 \times 10^{-17}$ cm^3 sec^{-1}. The boundary diffusion value is in good agreement with an earlier estimate made from kinetic experiments [18]. It is therefore concluded that the cellular phase transformation model represented by Equation 5 provides a reasonable description of the dealloying product morphology prior to aging. However, as seen in Fig. 8, the description is in error in its prediction of very fine pores and in its failure to account for the appearance of coarse pores. These effects arise from the small amount of coarsening which occurs during the course of the dealloying reaction. This coarsening process is now considered.

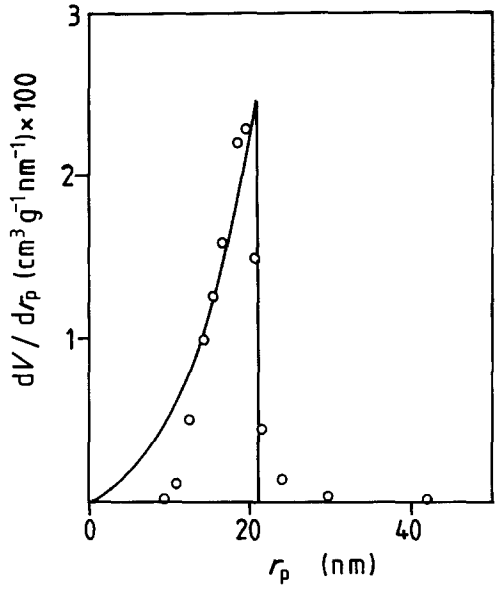

Figure 8 Pore size distribution after dealloying at 274 K for 90 h. The continuous curve shows the distribution calculated from the cellular phase transformation model assuming no coarsening occurs.

4.2. Coarsening of the rod structure

As is clear from Equations 7 and 10, the number density of copper rods produced in the initial dealloying process varies with position in the reacted rim. This implies the existence in the rod array of faults, such as terminations and confluences as shown schematically in Fig. 9. The volume concentration, f, for these faults is given by

$$f = -\frac{\partial N}{\partial x} \quad (11)$$

Similar faults have been observed in eutectics with lamellar and rod geometrics, and their dissolution behaviour found to produce coarsening of these structures [19, 20]. Because the volume fraction of copper within the rim is everywhere constant, the change in number of rods is accompanied by a change in rod size, as shown in Equation 9. This variation in surface curvatures will also drive a dissolution–reprecipitation process. However, this mechanism is less efficient, and, following the suggestion of Cline [20], the approximation that dissolution occurs only at rod terminations (where curvatures are highest) will be adopted. This rather special type of Ostwald ripening is now used to describe coarsening of the porous copper structure.

Rod terminations, or tips, are approximated as hemispheres having the same radius as that of the rod. It is assumed that copper dissolving from these tips diffuses a short distance through the liquid-filled pore space, and precipitates on the sides of nearby rods. If reprecipitation occurs at the same depth within the

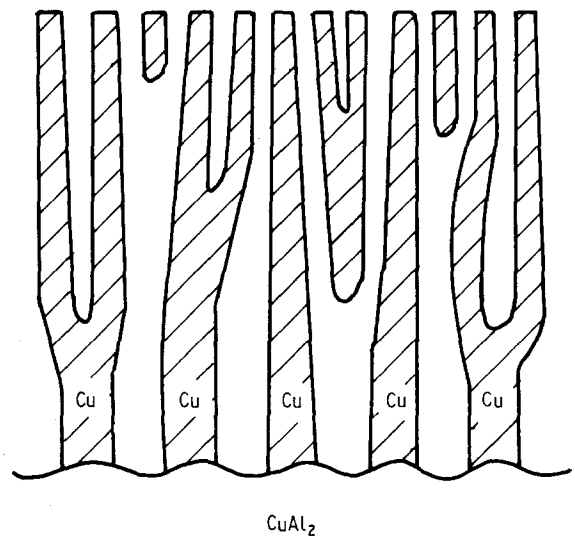

Figure 9 Schematic view of fault structure giving rise to variation in rod number density and spacing.

structure, it takes place on cylindrical surfaces having the same radius as the tip from which the copper dissolved. If the degree of supersaturation near the tips is small, the Gibbs–Thomson equation may be written in linear form

$$C_r - C^* = 2\sigma V_m C^*/r_{Cu}RT \quad (12)$$

where C_r is the solubility at a spherical surface with a radius of curvature r, and C^* is the solubility of a flat surface. For a cylindrical surface, the factor 2 is replaced by unity. Given that copper solubilities are low and that the regions of high solubility constitute a low volume fraction of the structure, then the rod tips will be surrounded by a gradient in concentration which approaches the bulk solution value at a distance S, where it equals the value appropriate to a cylindrical surface. A steady-state solution of the diffusion equation in spherical coordinates [21] may then be used to describe the copper dissolution flux

$$J = -\frac{\sigma V_m DC^*}{RT(1 - r_{Cu}/S)} \cdot \frac{1}{r_{Cu}^2} \quad (13)$$

From the spherical geometry of the tip, and the assumption that the rod radius is unchanged during dissolution, the rate at which the rod length, l, shortens is found from Equation 13 to be

$$\frac{dl}{dt} = \frac{-2\sigma V_m^2 DC^*}{RT(1 - r_{Cu}/S)} \cdot \frac{1}{r_{Cu}^2} \quad (14)$$

Combination of Equations 9, 10 and 14 then leads to an expression for the fault velocity, v,

$$v = \frac{dl}{dt} = \kappa N \quad (15)$$

where

$$\kappa = \frac{-2\sigma V_m^2 DC^* \pi}{RT(1 - r_{Cu}/S)f_{Cu}} \quad (16)$$

and it is noted that $r_{Cu}/S = (f_{Cu}/\pi)^{1/2}$ is a constant.

At a given position in the structure, the time rate of change in number density of rods is given by the flux of faults

$$\frac{\partial N}{\partial t} = -J_f = -vf = -\kappa N \frac{\partial N}{\partial x} \quad (17)$$

Substitution for v from Equation 15 followed by integration yields, for a given position,

$$\ln \frac{N}{N_0} = -\kappa \int_0^t f\,dt \quad (18)$$

where the subscript zero denotes time zero, i.e. after initial dealloying and before aging.

4.3. Numerical calculations

The partial differential Equation 17 was numerically solved by approximating f as constant for small time steps

$$\ln \frac{N(x, t + \Delta t)}{N(x, t)} = -\kappa f \Delta t \quad (19)$$

Initial values, $N(x, 0)$, were provided by Equations 7 and 10 and differentiation via Equation 11 yielded

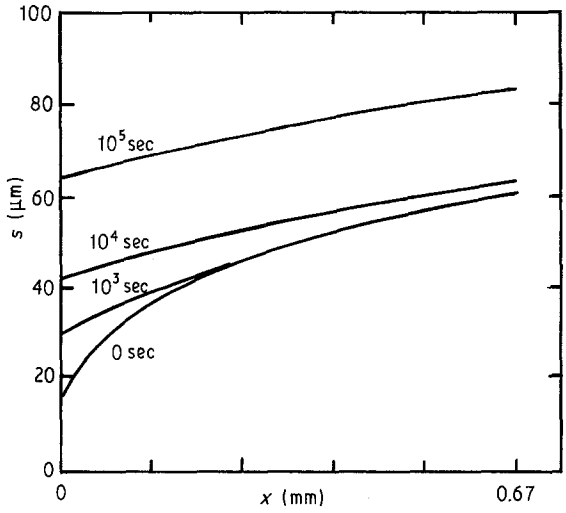

Figure 10 Calculated variation of spacing with position in the residue after indicated times of aging at 283 K of a residue produced at 274 K.

$f(x, 0)$. Stable solutions were obtained using time increments of 100 sec for each of 50 equal thickness concentric, cylindrical shells making up the leached zone. After each time increment, the new values for $f(x, t)$ were computed by differentiation using a five-point Lagrange interpolation formula [22]. The calculation was repeated until the total time equalled the desired aging time.

The variation of rod spacing with position in a residue produced at 274 K is shown in Fig. 10. The initial structure and its evolution during ripening at 283 K are shown, and an approach towards a rather uniform spacing is evident. The production of a remarkably uniform copper structure after aging has been verified by direct microscopic observation [6], and the model is therefore successful in this respect.

Pore size distributions were calculated by computing specific pore volumes, V_p, associated with discrete pore size ranges for each volume element of the structure, summing over the entire volume of the residue, and accumulating over the relevant range of pore sizes. The differential $\partial V_p/\partial r_p$ was then formed and compared with experimental data. Agreement was optimized with respect to agreement between measured and calculated values for r_p at which $\partial V_p/\partial r_p$ is maximum, using the unknown DC^* as an adjustable parameter.

Experimental and calculated values of r_p (max), the r_p value at which $\partial V_p/\partial r_p$ is maximum, are compared in Table III. Agreement is good for aging at 274 K, and for most of the data obtained at higher aging temperatures. Values of DC^* arrived at in achieving this agreement are also shown in Table III. Unfortunately, solubilities of copper in strongly alkaline solutions appear not to be well established [23]. Dissolved concentrations reported in Table I can be used to calculate values of D ranging from 8×10^{-6} cm^2 sec^{-1} at 274 K to 2×10^{-4} cm^2 sec^{-1} at 323 K. Although information on copper diffusion in strong alkaline solutions is lacking, these values appear reasonable for aqueous diffusion at ambient temperatures.

Pore size distributions measured after aging at 283 K of a residue produced at 274 K are shown in

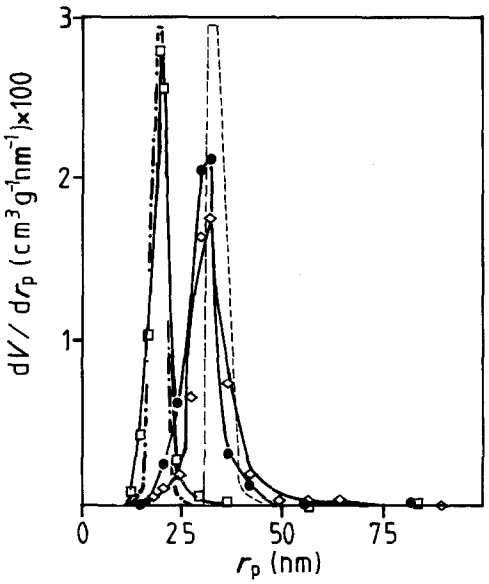

Figure 11 Comparison between measured and calculated pore size distributions after aging at 283 K of a residue produced at 274 K. (□ 5.3 h –·–·–, ◇ 72 h – – –, ● 169 h ——).

Fig. 11, along with distributions calculated from the model. It is seen that as the extent of ripening increases, the model description diverges from the measured distribution. This finding was quite general: with increasing degrees of coarsening, the pore size distributions always became much broader than was predicted from the present model. In view of the fact that the model also fails to predict correctly changes in r_p(max) after extended periods of aging, it must be concluded that it is of value only in the early stages of the ripening process.

At the highest temperature of 323 K the model breaks down as well: it predicts much too low a value of r_p(max) for short ripening times but adequate ones for longer times. Agreement for the shortest time can be achieved only with a value of DC^* six times higher, which leads to unreasonably high pore sizes for long ripening times.

The reason for these limitations is almost certainly a breakdown after some prolonged or very rapid coarsening has taken place, in the validity of the rod geometry description. As noted earlier, the pore morphology changes after some time, and their original parallel-sided form is lost. This means that the copper rods which define the pore size and shape must lose their geometrical perfection. This is likely due to spheroidization, a phenomeon observed with discontinuously precipitated rod structures [24], and preliminary indications of the development of such a morphology have been obtained by transmission electron microscopy of copper residues [25]. Under these conditions, the proposed model of dissolution only at rod tips clearly ceases to be applicable.

5. Conclusions

Dealloyed residues of copper have been found to coarsen during exposure to alkaline solutions at ambient temperature. It is concluded that the process is a type of Ostwald ripening which occurs via dissolution into and precipitation from the liquid phase. The grounds for this conclusion are as follows:

(i) The coarsening process proceeds independently of the dealloying process. The rate of coarsening increases with both temperature and alkali concentration.

(ii) Observed coarsening rates are consistent with liquid phase solubilities and diffusion coefficients for copper at the temperatures in question.

Early stages of the coarsening process are successfully described with the aid of a model based on dissolution from rod tips. This model breaks down at advanced stages of the process due to a structural change in the material, involving a loss of the rod geometry.

Acknowledgements

The work was supported by a grant from the Australian Research Grants Commission and the award (to ADT) of a Commonwealth Postgraduate Award. Fruitful discussions were held with J. S. Kirkaldy, G. R. Purdy and A. Bourdillon.

References

1. M. RANEY, US Patent 1 563 587 (1925).
2. J. B. FRIEDRICH, D. J. YOUNG and M. S. WAINWRIGHT, *J. Electrochem. Soc.* **128** (1981) 1840.
3. *Idem, ibid.* **128** (1981) 1845.
4. J. B. FRIEDRICH, M. S. WAINWRIGHT and D. J. YOUNG, *J. Catal.* **80** (1983) 1.
5. A. D. TOMSETT, D. J. YOUNG and M. S. WAINWRIGHT, *J. Electrochem. Soc.* **131** (1984) 2476.
6. J. SZOT, D. J. YOUNG, A. BOURDILLON and K. E. EASTERLING, *Phil. Mag. Lett.* **55** (1987) 109.
7. A. D. TOMSETT, H. E. CURRY-HYDE, M. S. WAINWRIGHT, D. J. YOUNG and A. J. BRIDGEWATER, *J. Appl. Catal.* **33** (1987) 119.
8. M. SATO and N. OHTA, *Bull. Chem. Soc. Jpn* **28** (1955) 182.
9. J. W. EVANS, M. S. WAINWRIGHT, A. J. BRIDGEWATER and D. J. YOUNG, *Appl. Catal.* **7** (1983) 75.
10. A. D. TOMSETT, M. S. WAINWRIGHT and D. J. YOUNG, *ibid.* **12** (1984) 43.
11. O. LEVENSPIEL, "Chemical Reaction Engineering", 2nd Edn (Wiley, New York, 1975).
12. D. TURNBULL, *Acta Metall.* **3** (1955) 55.
13. J. W. CAHN, *ibid.* **7** (1959) 18.
14. J. M. SHAPIRO and J. S. KIRKALDY, *ibid.* **16** (1968) 579.
15. B. SUNDQUIST, *ibid.* **16** (1968) 1413.
16. M. HILLERT, Monograph and Report Series No. 33 (Institute of Metals, London, 1969) p. 231.
17. D. H. EVERETT, in "The Structure and Properties of Porous Materials", edited by D. H. Everett and F. S. Stone, (Butterworths, London, 1958) p. 95.
18. D. J. YOUNG, in "Advances in Phase Transitions", edited by D. Embury and G. R. Purdy, (Pergamon Press, Oxford, 1988) pp. 116–130.
19. L. D. GRAHAM and R. W. KRAFT, *Trans. Metall. Soc. AIME* **236** (1966) 94.
20. H. E. CLINE, *Acta Metall.* **19** (1971) 481.
21. J. CRANK, "Mathematics of Diffusion" (Oxford University Press, Oxford, 1956).
22. R. H. PERRY and C. H. CHILTON (eds), "Chemical Engineers' Handbook", 5th edn (McGraw-Hill, Auckland, 1974) pp. 2–57.
23. O. J. KWOK, PhD Thesis, University of New South Wales (1974).
24. A. PEROVIC and G. R. PURDY, *Acta Metall.* **29** (1981) 53.
25. A. PEROVIC, G. R. PURDY, J. SKOGSMO and D. J. YOUNG, unpublished research (1988).

Received 21 February
and accepted 30 August 1989